

Theta vacuum and entanglement interaction in the three-flavor Polyakov-loop extended Nambu-Jona-Lasinio model

Takahiro Sasaki,^{1,*} Junichi Takahashi,^{1,†} Yuji Sakai,^{1,‡} Hiroaki Kouno,^{2,§} and Masanobu Yahiro^{1,¶}

¹*Department of Physics, Graduate School of Sciences, Kyushu University, Fukuoka 812-8581, Japan*

²*Department of Physics, Saga University, Saga 840-8502, Japan*

(Dated: November 8, 2018)

We investigate theta-vacuum effects on the QCD phase diagram for the realistic 2+1 flavor system, using the three-flavor Polyakov-extended Nambu-Jona-Lasinio (PNJL) model and the entanglement PNJL model as an extension of the PNJL model. The theta-vacuum effects make the chiral transition sharper. For large theta-vacuum angle the chiral transition becomes first order even if the quark number chemical potential is zero, when the entanglement coupling between the chiral condensate and the Polyakov loop is taken into account. We finally propose a way of circumventing the sign problem on lattice QCD with finite theta.

PACS numbers: 11.30.Rd, 12.40.-y

I. INTRODUCTION

The existence of instanton solution in quantum chromodynamics (QCD) requires the QCD Lagrangian with the theta vacuum:

$$\mathcal{L}_{QCD} = \bar{q}_f(\gamma_\nu D_\nu + m_f)q_f + \frac{1}{4}F_{\mu\nu}^a F_{\mu\nu}^a - i\theta \frac{g^2}{64\pi^2} \epsilon_{\mu\nu\sigma\rho} F_{\mu\nu}^a F_{\sigma\rho}^a \quad (1)$$

in Euclidean spacetime, where $F_{\mu\nu}^a$ is the field strength of gluon [1]. Theoretically the angle θ can take any arbitrary value between $-\pi$ and π . However, experiments indicate $|\theta| < 3 \times 10^{-10}$ [2, 3]. The Lagrangian is invariant under the combination of the parity transformation and the transformation $\theta \rightarrow -\theta$, so that parity (P) and charge-parity symmetry (CP) become exact only at $\theta = 0$ and $\pm\pi$; note that $\theta = -\pi$ is identical with $\theta = \pi$ because of the periodicity 2π in θ . Why should θ be so small? This long-standing puzzle is called the strong CP problem; see Ref. [4] and references therein for the detail.

For T higher than the QCD scale Λ_{QCD} , there is a possibility that θ is effectively varied to finite values depending on spacetime coordinates (t, x) , since sphalerons are so activated as to jump over the potential barrier between the different degenerate ground states [5]. If this happens, P and CP symmetries can be violated locally in high-energy heavy-ion collisions or the early Universe at $T \approx \Lambda_{QCD}$. Actually, it is argued in Refs. [6, 7] that θ may be of order 1 at the epoch of the QCD phase transition in the early Universe, whereas it vanishes at the present epoch [8–12]. This finite value of θ could be a new source of large CP violation in the early Universe and may be a crucial missing element for solving the puzzle of baryogenesis.

In the early stage of heavy-ion collision, the magnetic field is formed, while the effective $\theta(t, x)$ deviates the total number of particles plus antiparticles with right-handed helicity from those with left-handed helicity. As a consequence of this fact, an electromagnetic current is generated along the magnetic field, since particles with right-handed helicity move opposite to antiparticles with right-handed helicity. This is the so-called chiral magnetic effect [6, 13–15]. The chiral magnetic effect may explain the charge separations observed in the recent STAR results [16]. The thermal system with nonzero θ is thus quite interesting.

For vacuum with no temperature (T) and no quark-number chemical potential (μ), parity P is preserved when $\theta = 0$ [17], but is spontaneously broken when $\theta = \pi$ [18, 19]. The P violation, called the Dashen mechanism, is essentially non-perturbative, but the first-principle lattice QCD (LQCD) is not applicable for the case of finite θ because of the sign problem. Temperature (T) and/or quark-number chemical potential (μ) dependence of the mechanism has then been analyzed by effective models such as the chiral perturbation theory [7, 20–24], the Nambu-Jona-Lasinio (NJL) model [25–28] and the Polyakov-loop extended Nambu-Jona-Lasinio (PNJL) model [29, 30].

Using the two-flavor NJL model [31–33], Fujihara, Inagaki and Kimura made a pioneering work on the P violation at $\theta = \pi$ [25] and Boer and Boomsma studied this issue extensively [26, 27]. In the previous works [29, 30], we extended the formalism to the two-flavor PNJL and entanglement PNJL (EPNJL) models and investigated effects of the theta vacuum on the QCD phase diagram. Very recently similar analyses were made for the realistic case of 2+1 flavors by using the NJL model [28]. It is then highly expected that the finite- θ effect is investigated in the 2+1 flavor case by using the PNJL and EPNJL models that are more reliable than the NJL model.

If QCD with finite θ is analyzed directly with LQCD, one can get conclusive results on the theta vacuum. Here we consider a way of minimizing the sign problem in LQCD. For this purpose we transform the quark field q to the new one q' by the following $SU_A(3) \otimes U_A(1)$ transformation,

$$q_u = e^{i\gamma_5 \frac{\theta}{4}} q'_u, \quad q_d = e^{i\gamma_5 \frac{\theta}{4}} q'_d, \quad q_s = q'_s. \quad (2)$$

*sasaki@phys.kyushu-u.ac.jp

†takahashi@phys.kyushu-u.ac.jp

‡sakai@phys.kyushu-u.ac.jp

§kounoh@cc.saga-u.ac.jp

¶yahiro@phys.kyushu-u.ac.jp

The QCD Lagrangian is then rewritten into

$$\mathcal{L}_{QCD} = \sum_{l=u,d} \bar{q}'_l \mathcal{M}_l(\theta) q'_l + \bar{q}'_s \mathcal{M}_s q'_s + \frac{1}{4} F_{\mu\nu}^a F_{\mu\nu}^a \quad (3)$$

with the new quark field q' , where

$$\begin{aligned} \mathcal{M}_l(\theta) &\equiv \gamma_\nu D_\nu + m_l \cos(\theta/2) + m_l i\gamma_5 \sin(\theta/2), \\ \mathcal{M}_s &\equiv \gamma_\nu D_\nu + m_s. \end{aligned} \quad (4)$$

Only the Dirac operator $\mathcal{M}_l(\theta)$ has θ dependence in (3). The determinant of $\mathcal{M}_l(\theta)$ satisfies

$$\det \mathcal{M}_l(\theta) = (\det \mathcal{M}_l(-\theta))^*. \quad (6)$$

The sign problem is thus induced by the θ -odd (P -odd) term, $m_l i\gamma_5 \sin(\theta/2)$. The difficulty of the sign problem is expected to be minimized in the QCD Lagrangian of (3), since the θ -odd term includes the light quark mass m_l that is much smaller than Λ_{QCD} as a typical scale of QCD. This point is discussed in this paper.

In this paper, we analyze effects of the theta vacuum on the QCD phase diagram for the realistic case of 2+1 flavors by using the three-flavor PNJL [34] and EPNJL models [35]. Particularly, the three-flavor phase diagram is investigated in the μ - T plane with some values of θ . Through the analysis, we finally propose a way of circumventing the sign problem on LQCD calculations with finite θ .

This paper is organized as follows. In Sec. II, we recapitulate the three-flavor PNJL and EPNJL models. In Sec. III, numerical results are shown. Section IV is devoted to summary.

II. FORMALISM

The three-flavor PNJL Lagrangian with the θ -dependent anomaly term is obtained in Euclidean spacetime by

$$\begin{aligned} \mathcal{L} = & \bar{q}(\gamma_\nu D_\nu + \hat{m}_0 - \gamma_4 \hat{\mu})q \\ & - G_S \sum_{a=0}^8 [(\bar{q} \lambda_a q)^2 + (\bar{q} i\gamma_5 \lambda_a q)^2] \\ & + G_D \left[e^{i\theta} \det_{ij} \bar{q}_i (1 - \gamma_5) q_j + e^{-i\theta} \det_{ij} \bar{q}_i (1 + \gamma_5) q_j \right] \\ & + \mathcal{U}(\Phi[A], \Phi^*[A], T), \end{aligned} \quad (7)$$

where $D_\nu = \partial_\nu - i\delta_{\nu 4} A_4^a \lambda_a/2$ with the Gell-Mann matrices λ_a . The corresponding PNJL Lagrangian in Minkowski spacetime is shown in Refs. [29, 30]. The three-flavor quark fields $q = (q_u, q_d, q_s)$ have masses $\hat{m}_0 = \text{diag}(m_u, m_d, m_s)$, and the chemical potential matrix $\hat{\mu}$ is defined by $\hat{\mu} = \text{diag}(\mu, \mu, \mu)$ with the quark-number chemical potential μ . Parameters G_S and G_D denote coupling constants of the scalar-type four-quark and the Kobayashi-Maskawa-'t Hooft (KMT) determinant interaction [36, 37], respectively, where the determinant runs in the flavor space. The KMT determinant interaction breaks the $U_A(1)$ symmetry explicitly. Obviously, the theta-vacuum parameter θ has a periodicity of 2π . We then restrict θ in a period $0 \leq \theta \leq 2\pi$.

The gauge field A_μ is treated as a homogeneous and static background field in the PNJL model [29, 30, 34, 35, 38–52]. The Polyakov-loop Φ and its conjugate Φ^* are determined in the Euclidean space by

$$\Phi = \frac{1}{3} \text{tr}_c(L), \quad \Phi^* = \frac{1}{3} \text{tr}_c(\bar{L}), \quad (8)$$

where $L = \exp(iA_4/T)$ with $A_4/T = \text{diag}(\phi_r, \phi_g, \phi_b)$ in the Polyakov-gauge; note that λ_a is traceless and hence $\phi_r + \phi_g + \phi_b = 0$. Therefore we obtain

$$\begin{aligned} \Phi &= \frac{1}{3} (e^{i\phi_r} + e^{i\phi_g} + e^{i\phi_b}) \\ &= \frac{1}{3} (e^{i\phi_r} + e^{i\phi_g} + e^{-i(\phi_r+\phi_g)}), \\ \Phi^* &= \frac{1}{3} (e^{-i\phi_r} + e^{-i\phi_g} + e^{-i\phi_b}) \\ &= \frac{1}{3} (e^{-i\phi_r} + e^{-i\phi_g} + e^{i(\phi_r+\phi_g)}). \end{aligned} \quad (9)$$

We use the Polyakov potential \mathcal{U} of Ref. [41]:

$$\begin{aligned} \mathcal{U} = T^4 \left[-\frac{a(T)}{2} \Phi^* \Phi \right. \\ \left. + b(T) \ln(1 - 6\Phi\Phi^* + 4(\Phi^3 + \Phi^{*3}) - 3(\Phi\Phi^*)^2) \right] \end{aligned} \quad (10)$$

with

$$a(T) = a_0 + a_1 \left(\frac{T_0}{T}\right) + a_2 \left(\frac{T_0}{T}\right)^2, \quad b(T) = b_3 \left(\frac{T_0}{T}\right)^3. \quad (11)$$

The parameter set in \mathcal{U} is fitted to LQCD data at finite T in the pure gauge limit. The parameters except T_0 are summarized in Table I. The Polyakov potential yields a first-order deconfinement phase transition at $T = T_0$ in the pure gauge theory. The original value of T_0 is 270 MeV determined from the pure gauge LQCD data, but the PNJL model with this value of T_0 yields a larger value of the pseudocritical temperature T_c of the deconfinement transition at zero chemical potential than $T_c \approx 160$ MeV predicted by full LQCD [53–55]. Therefore we rescale T_0 to 195 (150) MeV so that the PNJL (EPNJL) model can reproduce $T_c = 160$ MeV [35].

a_0	a_1	a_2	b_3
3.51	-2.47	15.2	-1.75

TABLE I: Summary of the parameter set in the Polyakov-potential sector determined in Ref. [41]. All parameters are dimensionless.

Now the quark field q is transformed into the new one q' by (2) in order to remove θ dependence of the determinant interaction. As shown later, this transformation provides the thermodynamic potential Ω with a compact form and furthermore convenient to discuss the sign problem in LQCD. The present three-flavor PNJL model has 18 scalar and pseudoscalar condensates of quark-antiquark pair, but flavor off-diagonal condensates vanish for the system with flavor symmetric chemical potentials only [26, 27, 29, 30]. Since the quark-number

chemical potential considered in this paper is flavor diagonal, we can concentrate our discussion on flavor-diagonal condensates. Under the transformation (2), the flavor-diagonal quark-antiquark condensates, $\sigma_f = \bar{q}_f q_f$ and $\eta_f = \bar{q}_f i\gamma_5 q_f$, are transformed into $\sigma'_f = \bar{q}'_f q'_f$ and $\eta'_f = \bar{q}'_f i\gamma_5 q'_f$ as

$$\sigma_l = \cos\left(\frac{\theta}{2}\right)\sigma'_l + \sin\left(\frac{\theta}{2}\right)\eta'_l, \quad (12)$$

$$\eta_l = -\sin\left(\frac{\theta}{2}\right)\sigma'_l + \cos\left(\frac{\theta}{2}\right)\eta'_l, \quad (13)$$

$$\sigma_s = \sigma'_s, \quad (14)$$

$$\eta_s = \eta'_s \quad (15)$$

for $l = u, d$. The Lagrangian is then rewritten into

$$\begin{aligned} \mathcal{L} = & \bar{q}'(\gamma_\nu D_\nu + \hat{m}_{0+} + i\hat{m}_{0-}\gamma_5 - \gamma_4\hat{\mu})q' \\ & - G_S \sum_{a=0}^8 [(\bar{q}'\lambda_a q')^2 + (\bar{q}'i\gamma_5\lambda_a q')^2] \\ & + G_D \left[\det_{ij} \bar{q}'_i(1 - \gamma_5)q'_j + \det_{ij} \bar{q}'_i(1 + \gamma_5)q'_j \right] \\ & + \mathcal{U}(\Phi[A], \Phi^*[A], T) \end{aligned} \quad (16)$$

with

$$\begin{aligned} \hat{m}_{0+} &= \text{diag}(m_{u+}, m_{d+}, m_{s+}) \\ &= \text{diag}\left(\cos\left(\frac{\theta}{2}\right)m_u, \cos\left(\frac{\theta}{2}\right)m_d, m_s\right), \end{aligned} \quad (17)$$

$$\begin{aligned} \hat{m}_{0-} &= \text{diag}(m_{u-}, m_{d-}, m_{s-}) \\ &= \text{diag}\left(\sin\left(\frac{\theta}{2}\right)m_u, \sin\left(\frac{\theta}{2}\right)m_d, 0\right). \end{aligned} \quad (18)$$

Making the mean-field approximation, one can obtain the mean-field Lagrangian as

$$\begin{aligned} \mathcal{L}_{\text{MF}} = & \bar{q}'(\gamma_\nu D_\nu + M'_f + i\gamma_5 N'_f - \gamma_4\hat{\mu})q' \\ & + U_M + \mathcal{U}(\Phi[A], \Phi^*[A], T), \end{aligned} \quad (19)$$

where

$$M'_f = m_{f+} - 4G_S\sigma'_f + 2G_D(\sigma'_{f'}\sigma'_{f''} - \eta'_{f'}\eta'_{f''}), \quad (20)$$

$$N'_f = m_{f-} - 4G_S\eta'_f - 2G_D(\sigma'_{f'}\eta'_{f''} + \eta'_{f'}\sigma'_{f''}) \quad (21)$$

for $f \neq f'$, $f \neq f''$, $f' \neq f''$ and

$$\begin{aligned} U_M = & 2G_S \sum_{f=u,d,s} (\sigma'^2_f + \eta'^2_f) - 4G_D\sigma'_u\sigma'_d\sigma'_s \\ & + 4G_D(\sigma'_u\eta'_d\eta'_s + \eta'_u\sigma'_d\eta'_s + \eta'_u\eta'_d\sigma'_s). \end{aligned} \quad (22)$$

Performing the path integral over the quark field, one can obtain the thermodynamic potential Ω (per volume) for finite T and μ :

$$\begin{aligned} \Omega = & -2 \sum_{f=u,d,s} \int \frac{d^3\mathbf{p}}{(2\pi)^3} \left[N_c E_f \right. \\ & + \frac{1}{\beta} \ln [1 + 3\Phi e^{-\beta(E_f - \mu)} + 3\Phi^* e^{-2\beta(E_f - \mu)} + e^{-3\beta(E_f - \mu)}] \\ & + \frac{1}{\beta} \ln [1 + 3\Phi^* e^{-\beta(E_f + \mu)} + 3\Phi e^{-2\beta(E_f + \mu)} + e^{-3\beta(E_f + \mu)}] \left. \right] \\ & + U_M + \mathcal{U}(\Phi, \Phi^*, T) \end{aligned} \quad (23)$$

with $E_f = \sqrt{\mathbf{p}^2 + M'^2_f + N'^2_f}$.

The three-dimensional cutoff for the momentum integration is introduced [34], since this model is nonrenormalizable. For simplicity we assume the isospin symmetry for the u - d sector: $m_l \equiv m_u = m_d$. This three-flavor PNJL model has five parameters G_S , G_D , m_l , m_s and Λ . One of the typical parameter sets is shown in Table II. These parameters are fitted to empirical values of pion decay constant and π , K , η' meson masses at vacuum.

$m_l(\text{MeV})$	$m_s(\text{MeV})$	$\Lambda(\text{MeV})$	$G_S\Lambda^2$	$G_D\Lambda^5$
5.5	140.7	602.3	1.835	12.36

TABLE II: Summary of the parameter set in the NJL sector taken from Ref. [56].

For imaginary μ , Ω is invariant under the extended \mathbb{Z}_3 transformation [44],

$$\begin{aligned} e^{\pm\mu/T} &\rightarrow e^{\pm\mu/T} e^{\pm i\frac{2\pi k}{3}}, \quad \Phi \rightarrow \Phi e^{-i\frac{2\pi k}{3}}, \\ \Phi^* &\rightarrow \Phi^* e^{i\frac{2\pi k}{3}}, \end{aligned} \quad (24)$$

with integer k . This invariance ensures the Roberge-Weiss periodicity [57] in the imaginary chemical potential region [44]. Any reliable model should have this extended \mathbb{Z}_3 symmetry, when imaginary μ is taken in the model. This is a good test for checking the reliability of the model. The PNJL model has the extended \mathbb{Z}_3 symmetry [34, 44].

The four-quark vertex G_S is originated in a one-gluon exchange between quarks and its higher-order diagrams. If the gluon field A_ν has a vacuum expectation value $\langle A_0 \rangle$ in its time component, A_ν is coupled to $\langle A_0 \rangle$ and then to Φ through L . Hence we can modify G_S into an effective vertex $G_S(\Phi)$ depending on Φ [58]. The effective vertex $G_S(\Phi)$ is called the entanglement vertex and the model with this vertex is the EPNJL model. It is expected that Φ dependence of $G_S(\Phi)$ will be determined in future by the accurate method such as the exact renormalization group method [58–60]. In this paper, however, we simply assume the following form for $G_S(\Phi)$:

$$G_S(\Phi) = G_S[1 - \alpha_1\Phi\Phi^* - \alpha_2(\Phi^3 + \Phi^{*3})]. \quad (25)$$

This form preserves the chiral symmetry, the charge conjugation (C) symmetry [48] and the extended \mathbb{Z}_3 symmetry [44]. This entanglement vertex modifies the mesonic potential U_M , the dynamical quark masses M'_f and N'_f . This is the three-flavor version of the EPNJL model. In principle, G_D can depend on Φ , but Φ dependence of G_D is found to yield qualitatively the same effect on the phase diagram as that of G_S . Following Ref. [35], we neglect Φ dependence of G_D as a simple setup. In the present analysis, Φ dependence of G_D is thus renormalized in α_1 and α_2 . The EPNJL model thus constructed keeps the extended \mathbb{Z}_3 symmetry.

The parameters α_1 and α_2 in (25) are fitted to two results of LQCD at finite T ; one is the result of 2+1 flavor LQCD at $\mu = 0$ [61] that the chiral transition is crossover at the physical point and another is the result of degenerate three-flavor

LQCD at $\mu = iT\pi$ [62] that the order of the RW phase transition at the RW endpoint is first order for small and large quark masses and second order for intermediate quark masses. The parameter set (α_1, α_2) thus determined is located in the triangle region

$$\{-1.5\alpha_1 + 0.3 < \alpha_2 < -0.86\alpha_1 + 0.32, \alpha_2 > 0\}. \quad (26)$$

In this paper we take $\alpha_1 = 0.25$, $\alpha_2 = 0.1$ as a typical example, following Ref. [35].

The classical variables $X = \Phi$, Φ^* , σ_f and η_f are determined by the stationary conditions

$$\partial\Omega/\partial X = 0. \quad (27)$$

The solutions to the stationary conditions do not give the global minimum of Ω necessarily. There is a possibility that they yield a local minimum or even a maximum. We then have checked that the solutions yield the global minimum when the solutions $X(T, \mu, \theta)$ are inserted into (23).

III. NUMERICAL RESULTS

In this section we show numerical results for the original condensates (σ_f, η_f, Φ) , since this makes our discussion transparent. Under the parity transformation, σ_f, η_f and Φ are transformed into $\sigma_f, -\eta_f$ and Φ , respectively. This means that η_f is θ odd while σ_f and Φ are θ even, since the Lagrangian is invariant under the combination of the parity transformation and the transformation $\theta \rightarrow -\theta$. Thus η_f is an order parameter of the spontaneous parity breaking, while σ_f and Φ are approximate order parameters of the chiral and the deconfinement transitions, respectively. As an approximate order parameter of the chiral transition, $\sigma_l \equiv \sigma_u = \sigma_d$ is more proper than σ_s , since $m_l \ll m_s$.

A. Thermodynamics at $\mu = 0$

In this subsection, we consider the case of $\mu = 0$ where charge conjugation symmetry (C) is exact. Meanwhile, parity symmetry (P) is exact only at $\theta = 0, \pm\pi$, since $e^{i\theta}$ agrees with $e^{-i\theta}$ in (7) when $\theta = 0, \pm\pi$.

Figure 1 shows T dependence of σ_l, σ_s and Φ at $\theta = \mu = 0$, where σ_l and σ_s are normalized by $\sigma_0 = \sigma_l$ at $T = \mu = \theta = 0$. Here σ_l and Φ describe the chiral and deconfinement transitions, respectively. In the PNJL model of panel (a), the chiral restoration transition takes place after the deconfinement transition. In the EPNJL model of panel (b), meanwhile, both the transitions occur simultaneously. In the EPNJL model, σ_s decreases rapidly near the pseudocritical temperature $T_c = 160$ MeV, but goes down gradually above T_c . The rapid change of σ_s comes from that of Φ . For both the PNJL and EPNJL models, η_l and η_s are zero at any T . The P symmetry is thus always preserved when $\theta = 0$.

Figure 2 shows θ dependence of Ω and the order parameters at $T = \mu = 0$ in the EPNJL model; note that the EPNJL model agrees with the PNJL model at $T = 0$, since $G_S(\Phi) =$

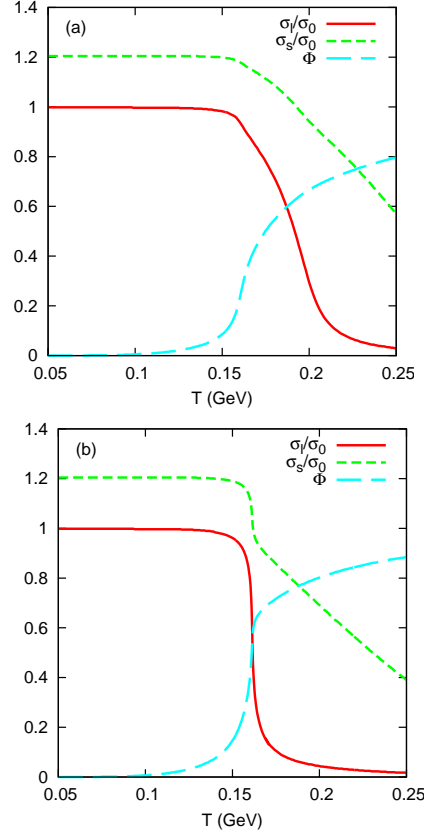


Fig. 1: T dependence of the order parameters at $\theta = 0$ and $\mu = 0$ in (a) the PNJL model and (b) the EPNJL model. The solid, dashed and dotted lines represent σ_l, σ_s and Φ , respectively, where σ_l and σ_s are normalized by $\sigma_0 = \sigma_l(T = \mu = \theta = 0)$.

G_S there because of $\Phi = 0$. As shown in panel (a), Ω is θ even and has a cusp at $\theta = \pi$. This indicates that a first-order phase transition takes place at $T = \mu = 0$ and $\theta = \pi$. As shown in panel (b), meanwhile, the η_f are θ odd, while σ_f and Φ are θ even. The condensate η_l and η_s have jumps at $\theta = \pi$, indicating that the first-order transition mentioned above is the spontaneous parity breaking. This is nothing but the Dashen phenomena [18].

Figure 3 shows θ dependence of the order parameters and the effective quark mass $\Pi_f \equiv \sqrt{M_f'^2 + N_f'^2}$ at $T = 163$ MeV and $\mu = 0$ in the EPNJL model. For this higher temperature, the Dashen phenomena do not take place at $\theta = \pi$. Actually η_l and η_s vanish there, although they become finite at $\theta \neq 0, \pi, 2\pi$ where P is not an exact symmetry. The other order parameters, σ_f and Φ , are smooth periodic functions of θ . The Polyakov loop Φ becomes maximum at $\theta = \pi$, since the effective quark mass Π_f becomes minimum and the thermal factor $\exp(-\beta E_f)$ is maximized in (23).

Figure 4 shows T dependence of the order parameters at $\theta = \pi$ and $\mu = 0$. Comparing this figure with Fig. 1, one can also see θ dependence of the order parameters. In the PNJL model of panel (a), $|\eta_l|$ and $|\eta_s|$ are finite below the critical temperature $T_P = 194$ MeV and vanish above T_P . Thus the

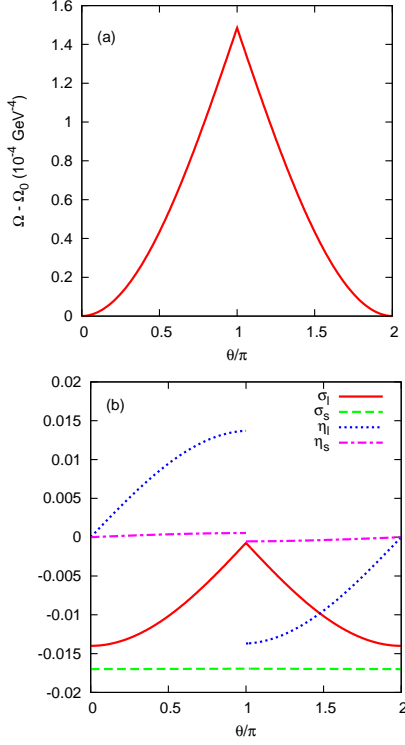


Fig. 2: θ dependence of (a) Ω and (b) the order parameters at $T = \mu = 0$ in the EPNJL model. In panel (a), $\Omega_0 \equiv \Omega(\theta = 0)$ is subtracted from Ω . See the legend for the definition of lines.

P symmetry is broken at smaller T , but restored at higher T . In the two-flavor PNJL model, this P restoration is second order [30]. This is the case also for the present 2+1 flavor PNJL model. The second order P restoration induces cusps in $|\sigma_l|$ and $|\sigma_s|$ when $T = T_P$, although the cusp is weak in $|\sigma_s|$. This propagation of the cusp can be understood by the extended discontinuity theorem of Ref. [47]. In the EPNJL model of panel (b), the P restoration occurs at $T_P = 158$ MeV as the first-order transition. The same property is seen in the two-flavor EPNJL model [30]. The first-order P restoration generates gaps in $|\sigma_l|$ and $|\sigma_s|$ when $T = T_P$, although the gap is tiny in $|\sigma_s|$. This propagation of the gap can be understood by the discontinuity theorem by Barducci, Casalbuoni, Pettini and Gatto [63]. Thus the Dashen phenomena are seen only at lower T , and the order of the P violation at the critical temperature T_P depends on the effective model taken.

Theoretical prediction on the critical temperature of the chiral transition at $\theta = 0$ and $\mu = 0$ and the P restoration at $\theta = \pi$ and $\mu = 0$ is tabulated in Table III. At $\theta = 0$, the chiral transition is crossover in all of the NJL, PNJL, and EPNJL models. At $\theta = \pi$, the order of the P restoration is first order in the EPNJL model, but it is second order in the PNJL and NJL models.

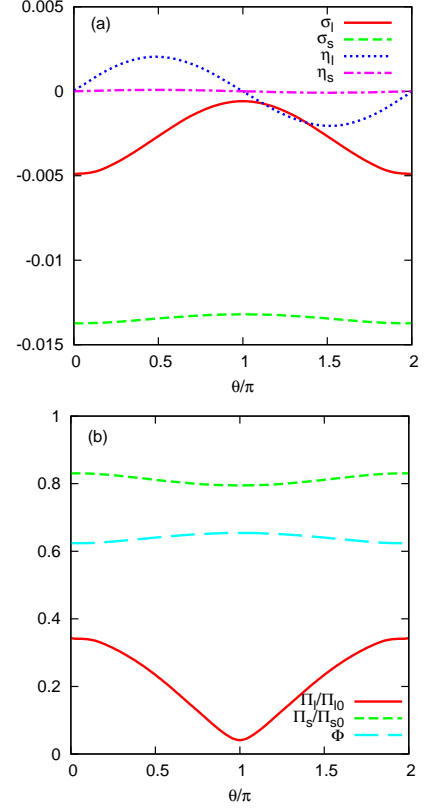


Fig. 3: θ dependence of (a) the order parameters and (b) the effective quark mass Π_f at $T = 163$ MeV and $\mu = 0$ in the EPNJL model. In panel (b), Π_f is normalized by the value at $T = \mu = \theta = 0$ and the normalized Π_f is compared with the Polyakov loop Φ . See the legend for the definition of lines.

Model	$\theta = 0$	$\theta = \pi$
NJL	177 (crossover)	170 (2nd order)
PNJL	200 (crossover)	194 (2nd order)
EPNJL	162 (crossover)	158 (1st order)

TABLE III: Theoretical prediction on the critical temperature of the chiral transition at $\theta = 0$ and $\mu = 0$ and the P restoration at $\theta = \pi$ and $\mu = 0$. The values are shown in units of MeV.

B. Thermodynamics at $\mu > 0$

In this subsection, we consider the case of $\mu > 0$ where C symmetry is not exact. In general, the relation $\Phi = \Phi^*$ is not satisfied for finite μ , although Φ and Φ^* are real [50]. This situation makes numerical calculations quite time-consuming. However, the deviation $\Phi - \Phi^*$ is known to be very small [50]. For this reason, the assumption $\Phi = \Phi^*$ has been used in many calculations. Therefore we use the assumption also in this paper.

Figure 5 represents T dependence of the order parameters at $\theta = \pi$ and $\mu = 300$ MeV in the PNJL and EPNJL models. The P restoration takes place at high T , since η_l and η_s are zero there. The critical temperature of the P restoration is

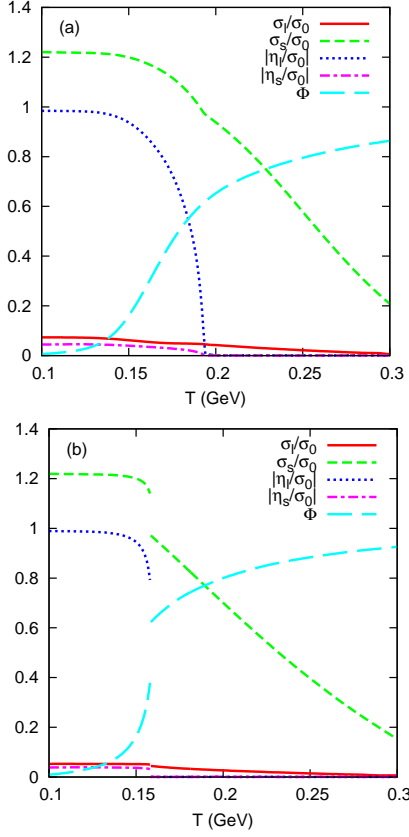


Fig. 4: T dependence of the order parameters at $\theta = \pi$ and $\mu = 0$ in (a) the PNJL model and (b) the EPNJL model. See the legend for the definition of lines.

$T_P = 110$ MeV for the PNJL model and $T_P = 99$ MeV for the EPNJL model. For $\mu = 300$ MeV, the order of the P restoration at $T = T_P$ is first order in both the PNJL and EPNJL models. Thus the quark-number chemical potential μ lowers T_P and makes the P restoration sharper.

Figure 6 shows the phase diagram of the chiral transition in the μ - θ - T space. The diagram is mirror symmetric with respect to the μ - T plane at $\theta = 0$, so the diagram is plotted only at $\theta \geq 0$. Panels (a) and (b) correspond to results of the PNJL and EPNJL models, respectively. In the μ - T plane at $0 \leq \theta < \pi$, the solid line stands for the first-order chiral transition, while the dashed line represents the chiral crossover. The meeting point between the solid and dashed lines is a critical endpoint (CEP) of second order. Point C is a CEP in the μ - T plane at $\theta = 0$ [32, 64]. For both the PNJL and EPNJL models, the location of CEP in the μ - T plane moves to higher T and lower μ as θ increases from 0 to π .

In the μ - T plane at $\theta = \pi$, P symmetry is exact and hence we can consider the spontaneous breaking of P symmetry in addition to the chiral transition. For the PNJL model of panel (a), both the first-order chiral transition and the first-order P restoration take place simultaneously, and the second-order P restoration and the chiral crossover coincide with each other. The first-order and the second-order P transition line are depicted by the solid and dashed lines, respectively. The meeting

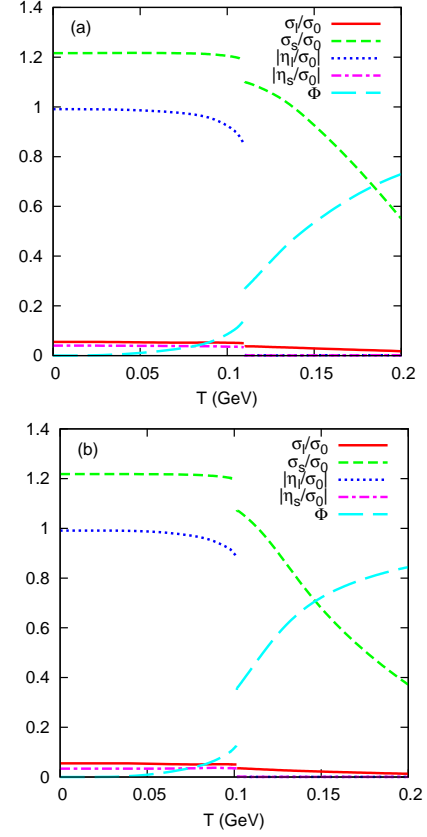


Fig. 5: T dependence of the order parameters at $\theta = \pi$ and $\mu = 300$ MeV in (a) the PNJL model and (b) the EPNJL model. See the legend for the definition of lines.

point A is a tricritical point (TCP) of the P -restoration transition. For the EPNJL model of panel (b), the chiral and the P restoration transition are always first order and hence there is no TCP.

In the PNJL model of panel (a), the dotted line from point C to point A is a trajectory of CEP as θ increases from 0 to π . Thus the second-order chiral transition line ends up with point A. This means that the CEP (point C) at $\theta = 0$ is a remnant of the TCP (point A) of P restoration at $\theta = \pi$. In the EPNJL model of panel (b), no TCP and then no CEP appears in the μ - T plane at $\theta = \pi$. The second-order chiral-transition line (dashed line) starting from point C never reaches the μ - T plane at $\theta = \pi$.

Figure 7 shows the projection of the second-order chiral-transition line in the μ - θ - T space on the μ - θ plane. The solid (dashed) line stands for the projected line in the EPNJL (PNJL) model. The first-order transition region exists on the right-hand side of the line, while the left-hand side corresponds to the chiral crossover region. The first-order transition region is much wider in the EPNJL model than in the PNJL model. In the EPNJL model, eventually, the chiral transition becomes first order even at $\mu = 0$ when θ is large.

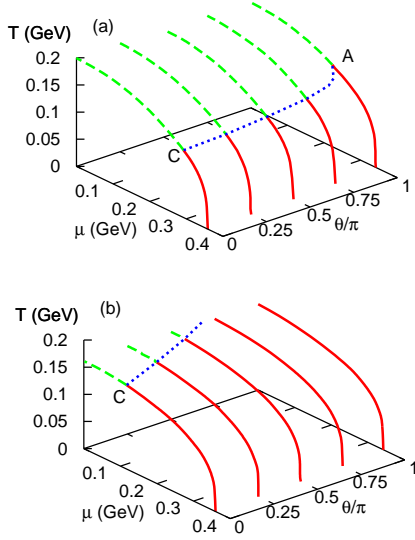


Fig. 6: Phase diagram of the chiral transition in the μ - θ - T space. Panel (a) shows a result of the PNJL model and panel (b) corresponds to a result of the EPNJL model.

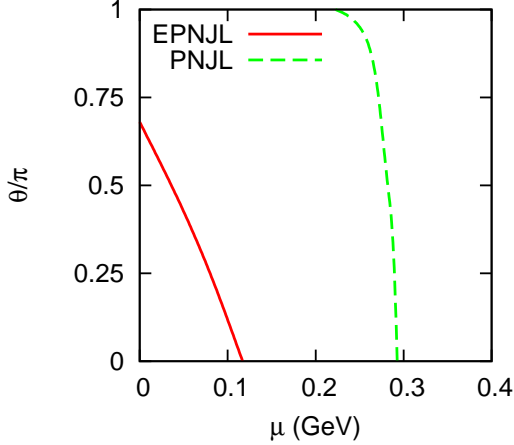


Fig. 7: The projection of the second-order chiral-transition line in the μ - θ - T space on the μ - θ plane. See the legend for the definition of line.

C. The sign problem on LQCD with finite θ

In the PNJL Lagrangian (16) after the transformation (2), θ dependence appears only at the light quark mass terms, $m_l \cos(\theta/2)$ and $m_l \sin(\theta/2)$. These terms are much smaller than Λ_{QCD} as a typical scale of QCD. This means that the condensates, σ'_l , σ'_s , η'_l and η'_s , have weak θ dependence. This statement is supported by the results of the PNJL calculations shown in Fig. 8.

The sign problem is induced by the θ odd $m_l \sin(\theta/2)$ term. The θ -odd (P -odd) condensates, η'_l and η'_s , are generated by the θ -odd mass term. One can see in Fig. 8 that the θ -odd condensates are much smaller than the θ -even condensates, σ'_l and σ'_s . This fact indicates that effects of the θ -odd mass term are negligible. Actually, if the term is neglected, the θ -even

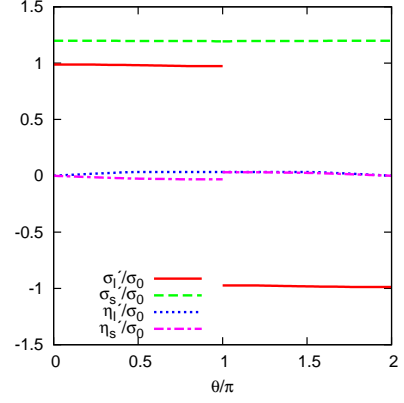


Fig. 8: θ dependence of the order parameters, σ'_l , σ'_s , η'_l and η'_s , at $T = \mu = 0$ calculated with the EPNJL model. See the legend for the definition of lines.

condensates change only within the thickness of line, while the θ -odd condensates vanish. The neglect of the θ -odd mass is thus a good approximation.

The validity of the approximation can be shown more explicitly in the following way. The θ -odd (P -odd) condensates, η'_l and η'_s , are zero at $\theta = 0$, since the θ -odd mass vanishes there. The weak θ dependence of η'_l and η'_s guarantees that η'_l and η'_s are small for any θ . Setting $\eta'_l = \eta'_s = 0$ in M'_l and N'_l leads to

$$M'_l = \cos\left(\frac{\theta}{2}\right)m_l - 4G_S\sigma'_l + 2G_D\sigma'_s\sigma'_l, \quad (28)$$

$$N'_l = \sin\left(\frac{\theta}{2}\right)m_l, \quad (29)$$

where $M'_l \approx \Lambda_{QCD}$ and $N'_l \approx m_l$. Since the thermodynamic potential is a function of $M'^2_l + N'^2_l$, the term N'^2_l is negligible compared with M'^2_l .

In LQCD, the vacuum expectation value of operator \mathcal{O} is obtained by

$$\langle \mathcal{O} \rangle = \int \mathcal{D}A \mathcal{O} (\det \mathcal{M}_l(\theta))^2 \det \mathcal{M}_s e^{-S_g} \quad (30)$$

$$= \int \mathcal{D}A \mathcal{O}' (\det \mathcal{M}'_l(\theta))^2 \det \mathcal{M}_s e^{-S_g} \quad (31)$$

with the gluon part S_g of the QCD action and

$$\mathcal{O}' \equiv \mathcal{O} \frac{(\det \mathcal{M}_l(\theta))^2}{(\det \mathcal{M}'_l(\theta))^2}, \quad (32)$$

where $\det \mathcal{M}'_l(\theta)$ is the Fermion determinant in which the θ -odd mass is neglected and hence has no sign problem. As mentioned above, one can assume that

$$\frac{\det \mathcal{M}_l(\theta)}{\det \mathcal{M}'_l(\theta)} \approx 1. \quad (33)$$

Thus the reweighting method defined by (31) may work well. In the θ -even mass, $m_l \cos(\theta/2)$, the limit of $\theta = \pi$ corresponds to the limit of $m_l = 0$ with m_s fixed. Although the limit is hard to reach, one can analyze the dynamics at least at small and intermediate θ .

IV. SUMMARY

We have investigated effects of the theta vacuum on the QCD phase diagram for the realistic 2+1 flavor system, using the three-flavor PNJL and EPNJL models. The effects can be easily understood by the $SU_A(3) \otimes U_A(1)$ transformation (2). After the transformation, the θ -odd mass, $m_l \sin(\theta/2)$, little affects the dynamics, so that the dynamics is mainly governed by the θ -even mass, $m_l \cos(\theta/2)$. In the θ -even mass, the increase of θ corresponds to the decrease of m_l with m_s fixed. This means that the chiral transition becomes strong as θ increases. This is true in the results of both PNJL and EPNJL calculations. Particularly in the EPNJL model that is more reliable than the PNJL model, the transition becomes first-order even at $\mu = 0$ when θ is large. This result is important. If the chiral transition becomes first order at $\mu = 0$, it will change the scenario of cosmological evolution. For example, the first-order transition allows us to think the inhomogeneous Big-Bang nucleosynthesis model or a new scenario of baryogenesis.

Using the fact that the θ -odd mass is negligible, we have proposed a way of circumventing the sign problem on LQCD with finite θ . The reweighting method by defined (31) may allow us to do LQCD calculations and get definite results on the dynamics of the θ vacuum.

Acknowledgments

The authors thank A. Nakamura, T. Saito, K. Nagata and K. Nagano for useful discussions. H.K. also thanks M. Imachi, H. Yoneyama, H. Aoki and M. Tachibana for useful discussions. T.S. and Y.S. are supported by JSPS. The numerical calculations were performed on the HITACHI SR16000 at Kyushu University and the NEC SX-9 at CMC, Osaka University.

-
- [1] C. G. Callan, R. F. Dashen, and D. J. Gross, Phys. Lett. **B63**, 334 (1976); J. Jackiw, and C. Rabbi, Phys. Rev. Lett. **37**, 172 (1976).
 - [2] C. A. Baker, et al., Phys. Rev. Lett. **97**, 131801 (2006).
 - [3] K. Kawarabayashi and N. Ohta, Nucl. Phys. **B175**, 477 (1980); Prog. Theor. Phys. **66**, 1789 (1981); N. Ohta, Prog. Theor. Phys. **66**, 1408 (1981); [Erratum-ibid. **67** (1982) 993].
 - [4] E. Vicari and H. Panagopoulos, Phys. Rept. **470**, 93 (2009).
 - [5] L. McLerran, E. Mottola and M. E. Shaposhnikov, Phys. Rev. D **43**, 2027 (1991).
 - [6] D. Kharzeev, and A. Zhitnitsky, Nucl. Phys. A **797**, 67 (2007).
 - [7] M. A. Metlitski, and A. R. Zhitnitsky, Nucl. Phys. **B731**, 309 (2005); Phys. Lett. B **633**, 721 (2006).
 - [8] R. D. Peccei and H. R. Quinn, Phys. Rev. D **16**, 1791 (1977).
 - [9] J. W. Kim, Phys. Rev. Lett. **43**, 103 (1979).
 - [10] M. A. Shifman A. I. Vainshtein and V. I. Zakharov, Nucl. Phys. B **166**, 493 (1980).
 - [11] A. R. Zhitnitsky, Sov. J. Nucl. Phys. **31**, 260 (1980).
 - [12] M. Dine W. Fischler and M. Srednicki, Phys. Lett. B **104**, 199 (1981).
 - [13] D. Kharzeev, Phys. Lett. B **633**, 260 (2006); D. Kharzeev, L. D. McLerran, and H. J. Warringa, Nucl. Phys. A **803**, 227 (2008).
 - [14] K. Fukushima, D. E. Kharzeev, and H. J. Warringa, Phys. Rev. D **78**, 074033 (2008).
 - [15] K. Fukushima, M. Ruggieri, and R. Gatto, Phys. Rev. D **81**, 114031 (2010).
 - [16] B. I. Abelev et al. [STAR Collaboration], Phys. Rev. Lett. **103**, 251601 (2009); Phys. Rev. C **81**, 054908 (2010).
 - [17] C. Vafa and E. Witten, Phys. Rev. Lett. **53**, 535 (1984).
 - [18] R. Dashen, Phys. Rev. D **3**, 1879 (1971).
 - [19] E. Witten, Ann. Phys. **128**, 363 (1980).
 - [20] P. di Vecchia, and G. Veneziano, Nucl. Phys. **B171**, 253 (1980).
 - [21] A. V. Smilga, Phys. Rev. D **59**, 114021 (1999).
 - [22] M. H. G. Tytgat, Phys. Rev. D **61**, 114009 (2000).
 - [23] G. Akemann, J. T. Lenaghan, and K. Splittorff, Phys. Rev. D **65**, 085015 (2002).
 - [24] M. Creutz, Phys. Rev. Lett. **92**, 201601 (2004).
 - [25] T. Fujihara, T. Inagaki, and D. Kimura, Prog. Theor. Phys. **117**, 139 (2007).
 - [26] D. Boer and J. K. Boomsma, Phys. Rev. D **78**, 054027 (2008).
 - [27] J. K. Boomsma and D. Boer, Phys. Rev. D **80**, 034019 (2009).
 - [28] B. Chatterjee, H. Mishra and A. Mishra, arXiv:1111.4061 [hep-ph](2011).
 - [29] H. Kouno, Y. Sakai, T. Sasaki, K. Kashiwa, and M. Yahiro, Phys. Rev. D **83**, 076009 (2011).
 - [30] Y. Sakai, H. Kouno, T. Sasaki, and M. Yahiro, Phys. Lett. B **705**, 349 (2011).
 - [31] Y. Nambu and G. Jona-Lasinio, Phys. Rev. **122**, 345 (1961); Phys. Rev. **124**, 246 (1961).
 - [32] M. Asakawa and K. Yazaki, Nucl. Phys. **A504**, 668 (1989).
 - [33] K. Kashiwa, H. Kouno, T. Sakaguchi, M. Matsuzaki, and M. Yahiro, Phys. Lett. B **647**, 446 (2007); K. Kashiwa, M. Matsuzaki, H. Kouno, and M. Yahiro, Phys. Lett. B **657**, 143 (2007).
 - [34] T. Matsumoto, K. Kashiwa, H. Kouno, K. Oda, and M. Yahiro, Phys. Lett. B **694**, 367 (2011).
 - [35] T. Sasaki, Y. Sakai, H. Kouno, and M. Yahiro, Phys. Rev. D **84**, 091901 (2011);
 - [36] G. 't Hooft, Phys. Rev. Lett. **37**, 8 (1976); Phys. Rev. D **14**, 3432 (1976); **18**, 2199(E) (1978).
 - [37] M. Kobayashi, and T. Maskawa, Prog. Theor. Phys. **44**, 1422 (1970); M. Kobayashi, H. Kondo, and T. Maskawa, Prog. Theor. Phys. **45**, 1955 (1971).
 - [38] P. N. Meisinger, and M. C. Ogilvie, Phys. Lett. B **379**, 163 (1996).
 - [39] K. Fukushima, Phys. Lett. B **591**, 277 (2004); Phys. Rev. D **77**, 114028 (2008).
 - [40] C. Ratti, M. A. Thaler, and W. Weise, Phys. Rev. D **73**, 014019 (2006).
 - [41] S. Rößner, C. Ratti, and W. Weise, Phys. Rev. D **75**, 034007 (2007).
 - [42] B. -J. Schaefer, J. M. Pawłowski, and J. Wambach, Phys. Rev. D **76**, 074023 (2007).
 - [43] K. Kashiwa, H. Kouno, M. Matsuzaki, and M. Yahiro, Phys. Lett. B **662**, 26 (2008).
 - [44] Y. Sakai, K. Kashiwa, H. Kouno, and M. Yahiro, Phys. Rev. D **77**, 051901(R) (2008); Phys. Rev. D **78**, 036001 (2008); Y. Sakai, K. Kashiwa, H. Kouno, M. Matsuzaki, and M. Yahiro,

- Phys. Rev. D **78**, 076007 (2008); K. Kashiwa, M. Matsuzaki, H. Kouno, Y. Sakai, and M. Yahiro, Phys. Rev. D **79**, 076008 (2009); K. Kashiwa, H. Kouno, and M. Yahiro, Phys. Rev. D **80**, 117901 (2009).
- [45] Y. Sakai, K. Kashiwa, H. Kouno, M. Matsuzaki, and M. Yahiro, Phys. Rev. D **79**, 096001 (2009);
- [46] T. Kähärä, and K. Tuominen, Phys. Rev. D **80**, 114022 (2009).
- [47] K. Kashiwa, M. Yahiro, H. Kouno, M. Matsuzaki, and Y. Sakai, J. Phys. G: Nucl. Part. Phys. **36**, 105001 (2009).
- [48] H. Kouno, Y. Sakai, K. Kashiwa, and M. Yahiro, J. Phys. G: Nucl. Part. Phys. **36**, 115010 (2009).
- [49] T. Sasaki, Y. Sakai, H. Kouno, and M. Yahiro, Phys. Rev. D **82**, 116004 (2010); Y. Sakai, H. Kouno, and M. Yahiro, J. Phys. G: Nucl. Part. Phys. **37**, 105007 (2010).
- [50] Y. Sakai, T. Sasaki, H. Kouno, and M. Yahiro, Phys. Rev. D **82**, 096007 (2010).
- [51] Y. Sakai, T. Sasaki, H. Kouno, and M. Yahiro, Phys. Rev. D **82**, 076003 (2010); arXiv:1104.2394 [hep-ph] (2011).
- [52] R. Gatto, and M. Ruggieri, Phys. Rev. D **83**, 034016 (2011).
- [53] W. Söldner, arXiv:1012.4484 [hep-lat] (2010).
- [54] K. Kanaya, arXiv:hep-ph/1012.4235 [hep-ph] (2010); arXiv:hep-ph/1012.4247 [hep-lat] (2010).
- [55] S. Borsányi, Z. Fodor, C. Hoelbling, S. D. Katz, S. Krieg, C. Ratti, and K. K. Szabo, arXiv:1005.3508 [hep-lat] (2010).
- [56] P. Rehberg, S.P. Klevansky and J. Hüfner, Phys. Rev. C **53**, 410 (1996); S.P. Klevansky, Rev. Mod. Phys. **64**, 649 (1992).
- [57] A. Roberge and N. Weiss, Nucl. Phys. **B275**, 734 (1986).
- [58] K.-I. Kondo, Phys. Rev. D **82**, 065024 (2010).
- [59] J. Braun, L. M. Haas, F. Marhauser, and J. M. Pawłowski, Phys. Rev. Lett. **106**, 022002 (2011); J. Braun, and A. Janot, arXiv:1102.4841 [hep-ph] (2011).
- [60] C. Wetterich, Phys. Lett. B **301**, 90 (1993).
- [61] Y. Aoki, G. Endrödi, Z. Fodor, S. D. Katz and K. K. Szabó, Nature **443**, 675 (2006).
- [62] P. de Forcrand and O. Philipsen, arXiv:1004.3144 [hep-lat](2010).
- [63] A. Barducci, R. Casalbuoni, G. Pettini, and R. Gatto, Phys. Lett. B **301**, 95 (1993).
- [64] A. Barducci, R. Casalbuoni, S. De Curtis, R. Gatto, and G. Pettini, Phys. Lett. B **231**, 463 (1989); A. Barducci, R. Casalbuoni, G. Pettini, and R. Gatto, Phys. Rev. D **49**, 426 (1994);